

# Bacterial Variability within an Iron-Silica-Manganese-rich Hydrothermal Mound Located Off-axis at the Cleft Segment, Juan de Fuca Ridge

Richard E. Davis,<sup>1</sup> Debra S. Stakes,<sup>2</sup> C. Geoffrey Wheat,<sup>3</sup> and Craig L. Moyer<sup>1</sup>

<sup>1</sup>Biology Department, Western Washington University, Bellingham, Washington 98225, USA

<sup>2</sup>Physical Sciences, Cuesta College, San Luis Obispo, California 93403, USA

<sup>3</sup>Global Undersea Research Unit, University of Alaska Fairbanks, Moss Landing, California 95039, USA

Terminal-restriction fragment length polymorphisms (T-RFLPs) and traditional clone library analysis were used to identify and assess the spatial variability of microbial communities within an active diffusely venting hydrothermal mound found 4 km off-axis at the Cleft Segment, Juan de Fuca Ridge. T-RFLP fingerprints were generated from three subsamples taken from different depths of a sediment core. The top and center subsamples were dominated by phylotypes clustering with the proposed  $\zeta$ -*Proteobacteria*. The bottom of the core was dominated by a phylotype clustering in the Nitrospina group within the  $\delta$ -*Proteobacteria*. Cluster analysis of T-RFLP fingerprints from the center of the core shows a similar community structure with those from iron-dominated microbial mat communities collected from NW Eifuku Seamount in the Mariana Island Arc and from Loihi Seamount, Hawaii. Our study demonstrates that off-axis diffuse hydrothermal activity generates microbial communities that can potentially affect their habitat through the differential precipitation of Fe-, Si-, and Mn-rich deposits.

**Keywords** biogeochemical cycling, biomineralization, community structure, iron-oxidizing bacteria

## INTRODUCTION

The Cleft Segment is the southernmost discreet spreading center of the Juan de Fuca Ridge (Figure 1). The highly symmetrical, intermediate-rate spreading center contains an axial collapse trough which runs the length of the center of the axial

valley and gives the segment its name (Embley et al. 1994). The rift valley walls are comprised of a series of major bounding faults, separated by blocks of oceanic crust that exhibit little or no deformation (Embley et al. 1994; Stakes et al. 2006). These blocks are almost entirely comprised of unfaulted, constructional pillow ridges, mounds, and hornitos, unlike the present axis which is dominated by sheetflows (Embley et al. 1983; Stakes et al. 2006).

There is observational and experimental evidence for small volumes of off-axis volcanism along eruptive fissures and from point-sources that appear related to the formation of rift-bounding faults (Chadwick et al. 1994; Massoth et al. 1994; Stakes et al. 2006). High-resolution Simrad EM300 bathymetry suggests that the flank topography is formed by these thick intact pillow flows that originate from faults within a few kilometers of the spreading axis and form flow fronts up to hundreds of meters high and lobate pillows up to tens of meters across (Stakes et al. 2006).

Off-axis venting in the form of small (6–8 meters tall) green mounds was first discovered on the Southern Cleft Segment in 2000 (Stakes et al. 2006). A small mound composed of bright green precipitate coated with a layer of Mn and draped in active microbial mats was found approximately 3 km east of the spreading axis during ROV Tiburon dive 178. These were described in detail during subsequent dives T179 and T457. This mound was composed of amorphous to poorly crystalline Fe-Si silicates and Fe-oxyhydroxides capped by cm thick layers of colloform Mn. Similar deposits were subsequently observed on dive T183 several km to the north suggesting a broad distribution of these vent sites on the east flank. In 2002, another small Fe-Si-Mn-rich mound was discovered on the western flank of the ridge during dive T460 (Stakes et al. 2003). This western Fe-Si-Mn-rich mound was found perched on a pillowed ridge on the edge of a ridge-parallel horst 4 km from the spreading axis. The interior of the 2 m high mound was composed of coarsely granular, poorly crystalline green Fe-silicate encrusting microbial filaments capped with a 5 cm thick red amorphous Fe layer that was itself capped by a thin layer of colloform Mn-oxide. A

Received 4 November 2008; accepted 3 February 2009.

We would like to thank the captain and crew of the of the R/V *Western Flyer* and the pilots of the ROV *Tiburon* for all their efforts during the collection of these samples. Funds from the Lucile and David Packard Foundation provided to MBARI supported the oceanographic expedition described in this study. This research was also supported in part by NOAA's Office of Ocean Exploration, the Office of Research and Sponsored Programs at Western Washington University and by National Science Foundation awards MCB-0348734 (to CLM) and GEBSN0056A (to RED).

Address correspondence to Craig L. Moyer, Biology Department, Western Washington University, Bellingham, WA 98225. E-mail: cmoyer@hydro.biol.wwu.edu



FIG. 1. Map showing the location of the Cleft Segment of the Juan de Fuca Ridge, northeast Pacific Ocean. Detailed bathymetric maps showing dive tracks and the location of the off-axis Fe-Si-Mn-rich mounds can be found in Stakes et al. (2006).

pushcore (Figure 2) of the mound successfully collected each of these layers and revealed that the mound was hollow on the interior. Thus these deposits represent a strongly zoned hydrothermal crust enclosing an active vent site.

This sediment pushcore sample provided an opportunity to determine the microbial composition in the hydrothermal sediments that are near but are considered off the central axis of a spreading center. Such sites must be common, based on the amount of conductive heat that must be removed from young crust (Mottl 2003), however only other two sites have been previously identified (Haymon et al. 2005; Fitzgerald and Gillis 2006) and only one sampled for microbial study (Huber et al. 2006). Initial microbial investigations of iron-rich hydrothermal sediments and microbial mats have resulted in the isolation of novel chemoautotrophic neutrophilic iron-oxidizing microbes (Emerson and Moyer 1997; Edwards et al. 2003; Emerson et al. 2007). These microbial isolates contribute greatly to the primary production at brine-dominated iron-rich hydrothermal vent systems. Furthermore, the importance of these microbes in hydrothermal systems with high concentrations of iron and/or manganese have received much less attention than sulfur-dominated habitats, yet their importance is becoming increasingly apparent in the global mineral cycling and in the weathering of seafloor basalts (Edwards et al. 2005; Kennedy et al.

2003a; Tebo et al. 2005; Templeton et al. 2005; Santelli et al. 2008).

In addition to elucidating the basic microbial ecology of hydrothermal sediments, a sediment core also provides an opportunity to study the spatial variability of microbial communities in a setting with increasing reduction potential downcore. Previously, researchers have been able to investigate the microbial spatial variability associated with active sulfide chimneys using culture-independent techniques (Schrenk et al. 2003; Takai et al. 2001); however, in these systems changes in microbial communities are driven by extreme temperature ( $\sim 350^{\circ}\text{C}$ ) and redox gradients resulting in substantially different microbial communities inhabiting microhabitats within the chimneys across an exceedingly small distance. In contrast, the push core from the Cleft mound was observed to be generally composed of a homogeneous material subject to a comparatively narrow temperature range spanning only a few degrees above ambient seawater ( $5.6^{\circ}\text{C}$  measured at interface: Table 1). Therefore, spatial variability of microbial communities within the sediment core can be correlated primarily with changes in redox conditions with depth.

The purpose of this study was to determine the phylogeny and spatial variability of microbial communities within hydrothermal sediments collected from an off-axis Fe-Si-Mn-rich mound. T-RFLP community fingerprinting (Liu et al. 1997) was used to track spatial variations with depth in the pushcore, and clone

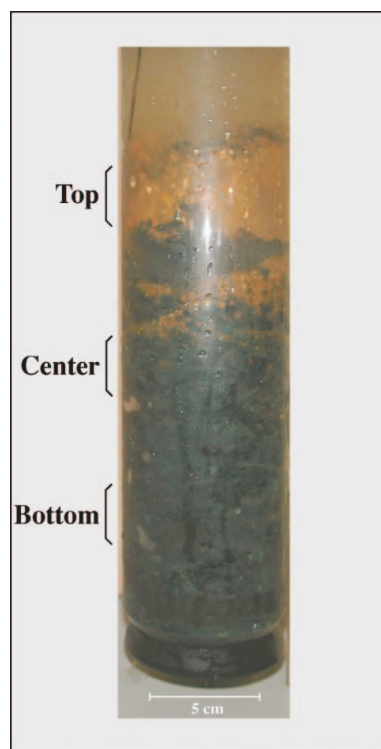


FIG. 2. Cleft mound pushcore 23 from *Tiburón* dive T460 with the locations of the top, center, and bottom subsamples. The location of the subsamples was determined by the obvious redox transition zones of the core.

TABLE 1  
Temperature, pH, and geochemical concentrations of ambient bottom seawater and of an off-axis Cleft mound

	Temperature (°C)	pH	Mg (mmol/kg)	SO <sub>4</sub> (mmol/kg)	Fe (μmol/kg)	Mn (μmol/kg)	Si (μmol/kg)
Bottom Seawater	1.8	7.90	52.6	28.1	0.00	0.00	185
Cleft Mound	5.6	7.54	51.9	27.3	0.94	9.73	241

library analysis of SSU rRNA genes was used to identify these communities and their phylogenetic positions (Moyer 2001). T-RFLP community fingerprinting is a sensitive genotyping method that is able to resolve ribotypes in a community with low to intermediate richness (Engebretson et al. 2003) and can be used in conjunction with traditional clone library analysis to identify and track these phylotypes through time and space. This study represents the first culture-independent study of a microbial community from the Cleft Segment of the Juan de Fuca Ridge.

## MATERIALS AND METHODS

### Sample Collection

Sediment pushcore 23 was collected in 2002 from a Fe-Si-Mn-rich hydrothermal mound located approximately 4 km west of the Cleft Axis (44.60°N, 130.44°W; depth 2291 m) on *ROV Tiburon* dive 460. Once aboard the ship, the pushcore was immediately subsampled into three sections (Figure 2), one from each visual redox transition zone, designated top, center, and bottom. Samples of microbial mats used for comparison were collected using a suction sampler with the DSRV submersible *Pisces V* at Loihi Seamount (Karl et al. 1988) in 2004 and with the *ROV ROPOS* at NW Eifuku Seamount (Davis and Moyer 2008) in 2004. All samples were aseptically transferred to sterile 50 ml centrifuge tubes and then immediately frozen and maintained at -80°C until DNA extraction was performed.

### Water Sampling and Chemical Analysis

Spring waters were collected in 750 ml Walden-Weiss titanium syringe samplers (Von Damm et al. 1985). Because of the slow (mm/s) and diffuse style of venting, inverted funnels were used to focus the flow before collection. Samples were filtered immediately upon recovery through 0.45 μm polycarbonate filters and stored in a variety of trace-metal clean, high-density polyethylene bottles with and without the addition of 6 N sub-boiled HCl to a pH of 1.8. Samples were measured immediately for pH and alkalinity. Alkalinity was determined by potentiometric Gran titration on 20 ml aliquots ( $1\sigma = 0.5\%$ ). Standard potential titration techniques were used to measure chlorinity ( $1\sigma = 0.2\%$ ). We used standard inductively coupled plasma atomic emission spectrometry (ICP-AES) to measure concentrations of the major and minor ions in seawater (in particular Mg, Mn, Fe and Si with  $1\sigma \cong 2\%$ ) with the exception of sev-

eral anions that were analyzed using ion chromatography (in particular sulfate with  $1\sigma = 2\%$ )

### SEM Preparation and Procedure

Sediment from the top of the pushcore was collected immediately after opening the core and preserved in formalin for morphological and mineralogical analysis. All scanning electron microscope (SEM) work was performed at the Microbeam Analytical Facility at the USGS Western Region campus at Menlo Park under the supervision of Robert Oscarson. Aliquots of sample were dispersed onto prepared mounts and dried prior to analysis using the JEOL 5800 SEM with secondary and backscatter detectors. The composition of individual particles was confirmed by use of the energy dispersive X-ray system.

### DNA Extraction

Total genomic DNA (gDNA) was extracted from each depth in triplicate using the FastDNA Spin Kit for Soil following the manufacturer's protocol (Q-biogene, Irvine, Ca). Extracted gDNA from each depth was pooled, cleaned, and concentrated using Montage PCR Centrifugal Filter Devices (Millipore, Bedford, MA). The gDNA was then quantified using OD 260/280 measurements on an HP diode-array spectrophotometer and was diluted to 10 ng DNA/μl using filter sterilized 10 mM Tris (pH 8.0).

### T-RFLP Preparation

Three replicate PCRs were performed, each using 50 ng of total gDNA and domain specific primers 68F and 1492R and conditions as previously described (Davis and Moyer 2008). The forward primer was labeled with 6-FAM (6-carboxyfluorescein) on the 5' end. The PCR products were visually assayed for size by 1% agarose gel electrophoresis against a 1-kb ladder DNA size standard. Only reaction mixtures yielding no amplification of the negative controls were used. The remaining fluorescently labeled PCR products were desalted using Montage PCR Centrifugal Filter Device. The PCR products (15 μl) were then partitioned into four aliquots and digested overnight at 37°C with 5 U of *Hae* III, *Hha* I, *Mbo* I, and *Rsa* I (New England Biolabs, Ipswich, MA) in a total volume of 30 μl. The restriction fragments were then desalted using superfine Sephadex G-75 (Amersham Biosciences, Uppsala, Sweden) and dehydrated. The fragments were resuspended in 15 μl formamide

and 0.33  $\mu$ l Genescan ROX-500 internal size standard (Applied Biosystems, Foster City, CA.), denatured by heating for 5 min at 95°C, and separated by capillary electrophoresis using an ABI 3100 genetic analyzer (Applied Biosystems).

### T-RFLP Analysis

The fluorescently labeled 5' terminal-restriction fragments were sized against the Genescan ROX-500 internal size standard using GeneMapper v3.7 (Applied Biosystems). Only fragments containing between 50 and 500 nucleotides were included in the analysis to only include fragments which can be accurately sized with the internal size standard and to prevent inclusion of primer-dimers in the analysis. Electropherograms were then imported into the program BioNumerics (Applied Maths, Sint-Martens-Latem, Belgium). Community fingerprints were compared in BioNumerics using the Pearson product moment correlation (Häne et al. 1993) and unweighted pair group method with arithmetic mean (UPGMA; Applied Maths) cluster analysis using the relative fluorescent proportions of each curve. The cophenetic correlation coefficient was calculated to assess the robustness of the cluster analysis groupings.

### Clone Library Construction

Five replicate PCRs were performed on the top core gDNA sample using identical PCR conditions and primers as with the T-RFLP amplification, only without 5' fluorochrome labeling. The PCR fragments were visually assayed for size and purity by gel electrophoresis as described here. The remaining sample was purified using a Montage PCR Centrifugal Filter Device and cloned with a QIAGEN PCR Cloning plus kit (QIAGEN, Hilden, Germany). All putative clones were streaked for isolation and the insert was assayed for size using PCR with the primers M13F and M13R and running the products against a 1 kb size standard by 1% agarose electrophoresis. Fifty-two clones were amplified using the primers M13F and M13R. The PCR products were then purified using Montage PCR Centrifugal Filter Device filters and diluted 2X with molecular biology grade water. The clones were then end-sequenced using the primers T7 and SP6 with BigDye Terminator v3.1 (Applied Biosystems). The Chao1 diversity estimate was calculated using the program DOTUR (Schloss and Handelsman 2005). Full-length clones were checked for chimeras using the Bellerophon server (Huber et al. 2004). Putative chimeras were further analyzed with the program Pintail (Ashelford et al. 2005) by comparing the putative chimera to any potential parent sequence.

### Phylogenetic Analysis

The full length clones were compared to sequences stored in GenBank using the BLAST algorithm (Altschul et al. 1990) and sequences with the greatest similarity to each clone were downloaded. These sequences and the full length clones were then imported into the ARB software environment and aligned to the SSU\_Jan04 database using the ARB fast aligner (Ludwig et al.

2004). Additional sequences were selected in the database and exported to the sequence alignment program Bioedit (Hall 1999) for additional alignment editing. Phylogenetic analyses were restricted to regions of moderately to highly conserved nucleotide positions that were unambiguously aligned for all sequences. Phylogenetic placements were calculated using fastDNAm1 version 1.2.2 (Olsen et al. 1994) using the general two-parameter model of evolution (Kishino et al. 1989) and allowing for the global swapping of branches. Using these parameters, the search for an optimal tree was repeated until the best log likelihood tree was calculated in at least three independent tree calculations. Each phylogenetic tree was bootstrapped 100 times allowing for the global swapping of branches. The search for each bootstrap was repeated until the best log likelihood score was calculated for at least two independent bootstrap calculations.

### Nucleotide Sequence Accession Numbers

Full length SSU rRNA sequences have been deposited in GenBank under accession numbers DQ832632 to DQ832646.

## RESULTS

### Geochemistry Results

Several major and minor ions were analyzed from diffuse fluids emanating from the Cleft mound. These included pH, alkalinity, chlorinity, sulfate, Sr, Li, Na, Ca, K, Mg, Ba, B, Fe, Mn and Si. The ones determined to be notably different from ambient bottom seawater and potentially having an impact on the microbiology are shown in Table 1.

### Microscopy Results

An SEM survey of the particles within the pushcore suggests a variety of hydrothermal precipitates and microbial filaments intermixed with pelagic diatoms and coccoliths (Figure 3). Photosynthetic-derived detritus consisted of siliceous diatom fragments that have passed through the water column and were resistant to microbial degradation. Iron filaments were similar to structures found in microbial mats from Loihi Seamount (Karl et al. 1988; Emerson and Moyer 2002) and from hydrothermal vents at Axial Volcano, Juan de Fuca Ridge (Kennedy et al. 2003b). These filaments have been shown to be biogenically produced by neutrophilic iron-oxidizing bacteria isolated from iron-rich water (Kucera et al. 1957) and from iron-dominated microbial mats (Emerson et al. 2007). Elevated temperature as well as the reduction in pH with enhanced concentrations of iron, manganese and silica relative to background seawater were shown in the diffusely venting mound fluids (Table 1).

### T-RFLP and Clone Library Results

T-RFLP fingerprints indicate low to intermediate community richness and low community evenness throughout the core (Figure 4). The top of the core contained the greatest community richness with 11.9 average terminal-restriction fragments

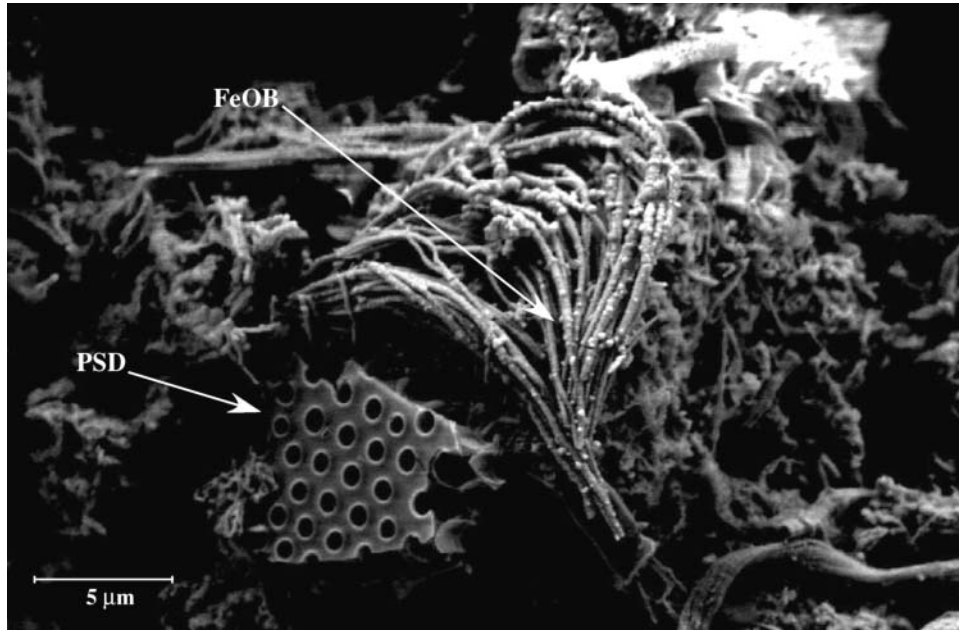


FIG. 3. Scanning electron micrograph of the top of the Cleft mound pushcore showing photosynthetic detritus (PSD) and iron filaments likely formed by iron oxidizing bacteria (FeOB).

(T-RFs) per digest, followed by the center of the core with 11.4 average T-RFs per digest, and then the bottom of the core with 4.3 average T-RFs per digest (Table 2). The dominant peaks shifted in each of the three core samples, indicating the dominant phylotype in the core changed with depth. Although the populations change dramatically throughout the depth of the sediments, nearly all peaks present in the bottom and center sections of the core were also present in the top of the core (Figure 4).

The moderate diversity throughout the core (i.e., exhibited by the three subsamples) and the presence of nearly all of the T-RF peaks in the top sample allowed for the construction of a single SSU rRNA clone library from the top sample and for the extrapolation of this library to identify the majority of phylotypes also detected in the center and bottom core samples. The clone library consisted of 25%  $\zeta$ -*Proteobacteria*, 19% *Planctomycetes*, 17% *Bacteroidetes*, 13%  $\alpha$ -*Proteobacteria*, 13%  $\gamma$ -*Proteobacteria*, 10%  $\delta$ -*Proteobacteria*, and 3%  $\epsilon$ -*Proteobacteria*. The library had a Chao1 diversity estimate (Chao 1984) of 37 with a 97% similarity cutoff. Predicted 5' terminal-restriction fragments

(T-RFs) were identified for each clone *in silico*. Clones that had unique restriction fragments and were identifiable on the T-RFLP electropherograms for each restriction digest were fully sequenced.

The top of the core was dominated by CM25 (Table 2), a phylotype most closely related a clone found at the brine-seawater interface of the Kebrit Deep in the Red Sea (Figure 5; Eder et al. 2001). This clone is also closely related to *Mariprofundus ferrooxydans*, a neutrophilic obligate chemoautotrophic iron-oxidizing bacteria that has recently been isolated from a hydrothermal vent associated microbial mat (Emerson et al. 2007). Other relatively abundant phylotypes were represented by clones CM3 and CM59, which clustered within the methanotrophic group of the  $\gamma$ -*Proteobacteria* subdivision (Figure 5). All known isolates from this group utilize C1 compounds as both energy and carbon sources (Bowman et al. 1995). The top of the core also contained numerous phylotypes related to heterotrophic bacteria lineages. These bacteria include members of the  $\alpha$ -*Proteobacteria*,  $\gamma$ -*Proteobacteria*, *Planctomycetes* and the *Bacteroidetes* (Figure 5; Figure 6).

TABLE 2  
Sediment color, average number of T-RFs per digest, dominant clone-type, and phylogenetic affiliation from each of the subsamples of the Cleft mound pushcore

Subsample	Sediment color	Average T-RFs per digest	Dominant clone-type	Phylogenetic affiliation
Top	Orange	11.9	CM25	Mariprofundus group
Center	Orange/Green	11.4	CM2	Mariprofundus group
Bottom	Green	4.3	CM34	Nitrospina group

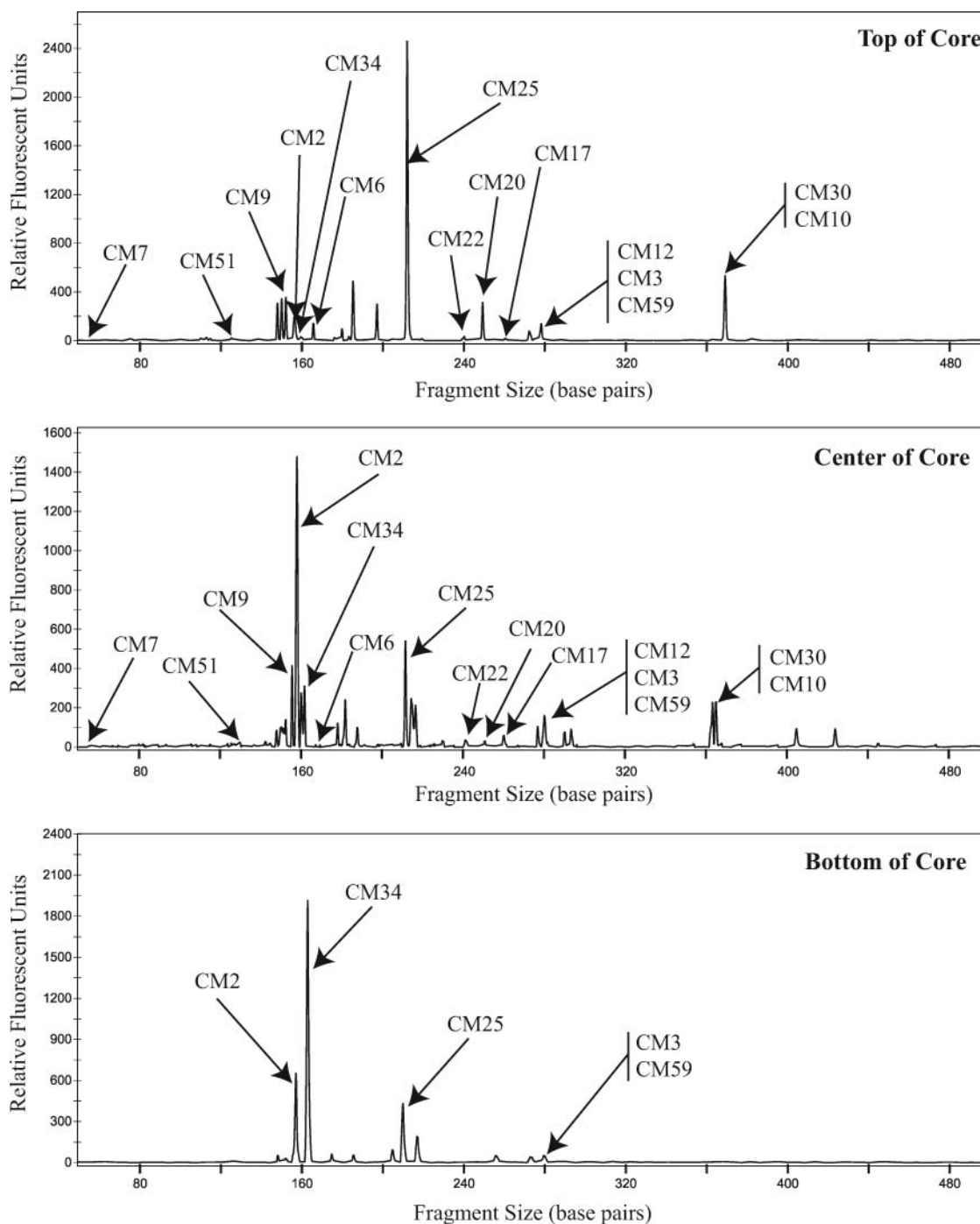


FIG. 4. Representative (*Hae* III) T-RFLP electropherogram of the bacterial communities from the three subsections of the Cleft mound pushcore. Arrows indicate the 5' T-RFs of clones found in the clone library.

The center sample of the core contained all of the phylotypes detected in the top sample with nearly the same richness (Table 1), however it was dominated by the clone CM2 phylotype (Table 1; Figure 5). Clone CM2 clusters within the  $\zeta$ -*Proteobacteria* and is most closely related to an uncultured clone PVB OTU 4, which was found at a hydrothermal

vent microbial mat at Loihi Seamount, Hawaii (Moyer et al. 1995).

The bottom sample of the core had the least amount of diversity, in terms of richness and evenness, when compared to the top and center of the core (Table 1). None of the putative heterotrophs from the top and center samples were



FIG. 5. Maximum-likelihood phylogenetic tree showing the evolutionary placement of clones belonging to the *Proteobacteria* division of Bacteria, including the proposed  $\zeta$ -*Proteobacteria* subdivision. Scale bar represents 5 nucleotide substitutions per 100 positions.

detected in the bottom core (Figure 4). The dominant phylotype present in the bottom of the core was represented by CM34. Clone CM34 clusters deeply within the Nitrospina group of the  $\delta$ -*Proteobacteria* (Figure 5). The sample from the bottom of the core also contained relatively abundant phylotypes (to a lesser degree) represented by  $\zeta$ -*Proteobacteria* phylotypes CM2 and CM25 as well as the methanotrophic group clones CM3 and CM59 (Figure 4 and Figure 5).

### Cluster Analysis Results

Cluster analysis of T-RFLP fingerprints shows a strong clustering with respect to the similarity of the microbial community composition from the center of the core with communities from iron-dominated hydrothermal vent microbial mats from

NW Eifuku Seamount in the Mariana Island Arc and from Loihi Seamount, Hawaii (Figure 7). Microbial communities from the top and bottom of the core do not group within the iron-dominated microbial mat cluster nor do they strongly cluster with each other (Figure 7).

### DISCUSSION

Systematic geological observations and off-axis sampling of the Cleft Segment of the Southern Juan de Fuca Ridge made with the MBARI ROV *Tiburon* have provided a unique perspective on the crustal evolution along this typical moderate spreading-rate ridge (Stakes et al. 2006). The rift valley walls are comprised of a series of major bounding faults, separated by blocks of oceanic crust that exhibit little or no deformation.

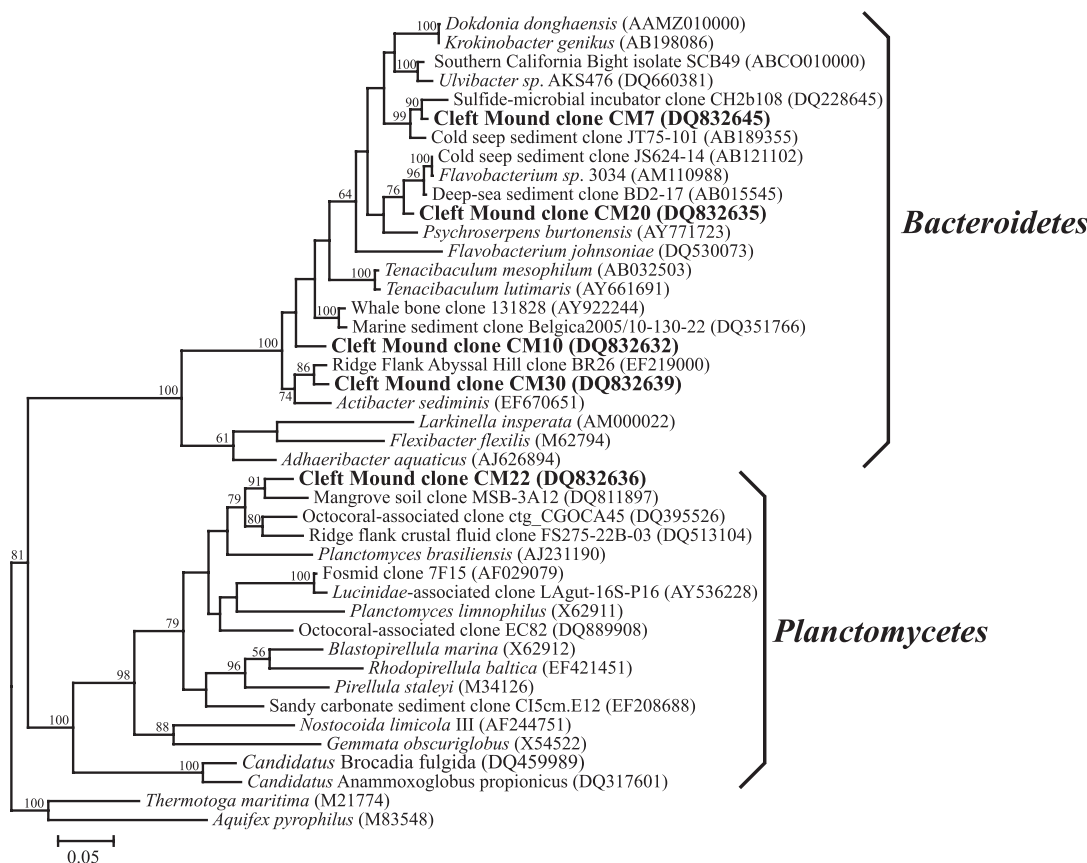


FIG. 6. Maximum-likelihood phylogenetic tree showing the evolutionary placement of clones belonging to the *Planctomyces* and the *Cytophaga-Flexibacter-Bacteroidetes* (CFB) divisions of Bacteria. Scale bar represents 5 nucleotide substitutions per 100 positions.

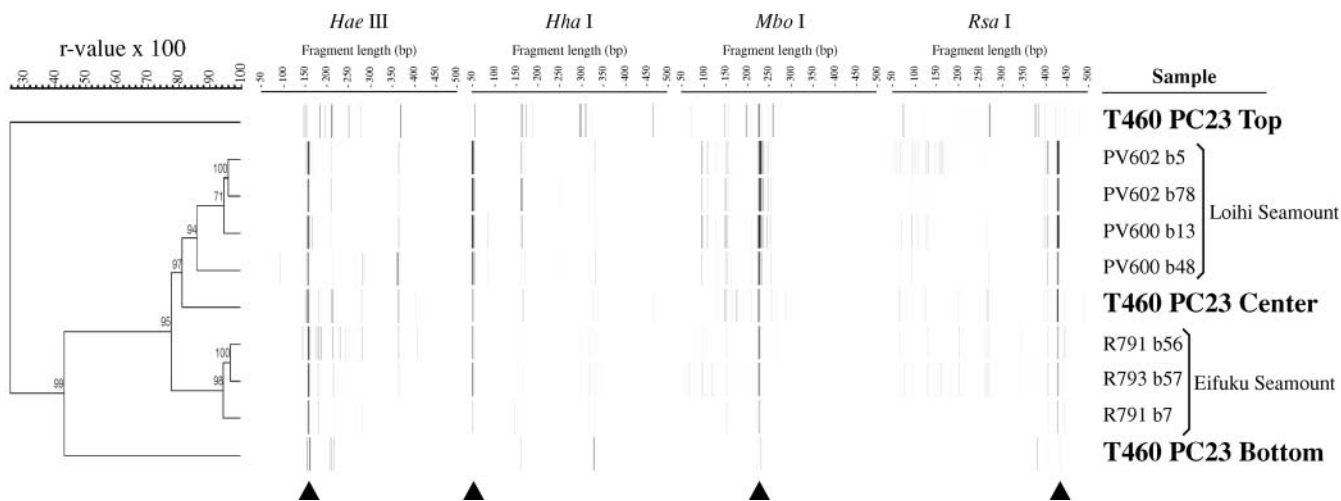


FIG. 7. UPGMA/product-moment cluster analysis of T-RFLP bacterial community fingerprints from the three Cleft mound subsamples and from iron-dominated microbial mats from Loihi and NW Eifuku Seamounts using four restriction digest treatments of which images are shown in the center panel. Triangles at bottom indicate T-RFs associated with the center core dominant  $\zeta$ -Proteobacteria phylotype (CM 2). T-RF scales range from 50 to 500 base pairs. Dendrogram scale bar units are r value  $\times$  100. Numbers at the nodes indicate the cophenetic correlation value of the cluster.



There is observational evidence for small volumes of off-axis volcanism along eruptive fissures and from point-sources that appear related to the formation of rift-bounding faults. The contact between the massive pillowed units and the older sheet flows (~3 km to the east and west) is clearly delineated both by sediment cover and by lava flow morphology. Associated with these structural constraints is evidence for low temperature off-axis venting in the form of Fe-rich precipitates, some of which included active venting at temperatures up to 20°C above ambient.

Because of the minimal hydrothermal fluid flow in the vicinity of pushcore 23, we were unable to obtain a fluid sample there. However, because of the ubiquitous nature of hydrothermal deposits, which were found on each off-axis dive, hydrothermal fluids that we collected from a similar geologic setting with faster fluid egress is likely to be representative of those fluids that form all such deposits in the area. We collected hydrothermal fluids that were only a few degrees Celsius warmer than background and were diluted by bottom seawater during sampling; nonetheless, a few geochemical trends are apparent. Concentrations of both Mg and sulfate (Table 1) in hydrothermal fluids were less than that of bottom seawater, in contrast to concentrations of Si, Mn, and Fe which are greater in hydrothermal fluids (Table 1). Concentrations of K and Li as well as chlorinity were not different from bottom seawater (data not shown). Collectively, these data (along with the observation that there were no sediments across the entire ridge axis in this region that might support sulfate reduction) confirm that the source fluid was once a high temperature fluid (>150°C) that has cooled, mixed with seawater, and reacted with basalt under cool (<150°C) conditions before venting at the seafloor where reduced Fe and Mn can be utilized by microbial communities.

T-RFLP analysis of the microbial communities in the sediment core showed a strong bacterial community shift between each of the sediment core subsamples. The top and center core samples had similar community diversity in terms of taxa richness and evenness (Table 2), however the relative phylotype proportions and the dominant phylotype shifted between the top and the center of the core. The bottom of the core differed from the top and center in taxa diversity and composition (Table 2; Figure 4), indicating a distinct change in habitat with depth. This change is most likely a result of increased redox potential and lack of dissolved oxygen with increasing depth.

The top and center of the mound were dominated by members of the  $\zeta$ -*Proteobacteria*. This unique monophyletic group contains only clones and isolates found from areas with sharp redox transition zones, such as the brine-seawater interface in the Red Sea (Eder et al. 2001) and hydrothermal vents at Loihi Seamount (Emerson et al. 2007) and Guaymas Basin (Dhillon et al. 2003). *Mariprofundus ferrooxydans* is the only known cultured representative of this group, which has been proposed as a novel subdivision of the *Proteobacteria*, the  $\zeta$ -*Proteobacteria* (Emerson et al. 2007). *Mariprofundus ferrooxydans* is a mi-

croaerophilic obligate chemoautotrophic bacterium which oxidizes ferrous iron to insoluble ferric oxides under near-neutral pH conditions (Emerson et al. 2007). The morphology of these microbial iron oxides is similar to those observed in SEM images of sediments from the top of the core (Emerson and Moyer 2002; Figure 3).

The dominance of clones represented by the  $\zeta$ -*Proteobacteria* combined with the elevated concentrations of iron and manganese in vent fluids indicate a metabolic dominance of neutrophilic and possibly chemoautotrophic iron and manganese oxidation in the top and center of the core. No phylotypes closely related to known Mn-oxidizing bacteria were found, suggesting the Mn oxides found on the Cleft mound were deposited by bacteria other than those that have already been cultured. Although methane was not measured at the Cleft mound, the presence of phylotypes closely related to methanotrophic cultures (Figure 5) suggests that methane oxidation may be an important autotrophic metabolism in the community. The presence of a high number of phylotypes closely related to cultured oligotrophic bacteria in these samples (Figure 5; Figure 6) indicate that the uptake of dissolved organic carbon (DOC) along with the degradation of particulate organic carbon (POC) was also a dominant metabolism in these communities. These communities may obtain organic carbon from either the autochthonous chemoautotrophic community found in the mound or from photosynthetic detritus from the upper water column (Figure 3).

The bottom of the core is dominated by clone CM34 (Table 2; Figure 4) that clusters deeply within the Nitrospina group of the  $\delta$ -*Proteobacteria* subdivision (Figure 5), which are not derived directly from any known photosynthetic ancestry as are other nitrite-oxidizing bacteria (Teske et al. 1994). Although the only isolated member of the Nitrospina group is the aerobic nitrite-oxidizing bacterium *Nitrospina gracilis* (Watson et al. 1971) there are numerous *Nitrospina* environmental clones that are found associated with deep-sea sediments (Li et al. 1999) and hydrothermal microbial mats (Davis and Moyer 2008), suggesting a wider diversity of metabolic strategies exist within the Nitrospina group than have been discovered through culturing techniques. Other anaerobic metabolisms, such as sulfate- and iron-reduction, have been found within cultured deep-sea sediments associated  $\delta$ -*Proteobacteria* (Devereux et al. 1994; Lovley 1997) and may indicate an alternative dominant metabolism in the bottom core sample.

The close T-RFLP fingerprint clustering of the center of the Cleft mound core sample coupled with known iron-dominated microbial communities sampled from a variety of hydrothermal systems (Figure 7) suggests a strong correlation among these microbial communities. This strong correlation of the microbial communities implies a similarity among the habitats in which these communities reside. Since the center of the mound was sampled at the redox transition between the oxidized top section and the highly reduced bottom section, iron-dominated microbial mats likely must reside within certain redox conditions.

These redox conditions can be enhanced and maintained by the microbial community through the formation of mucopolysaccharides and iron-manganese crusts (Emerson et al. 1994; Brendel et al. 1995). Conversely, since the microbial communities from the top and bottom pushcore subsamples do not cluster with the communities from the microbial mat samples, they may reside in novel habitats that may be common in diffuse venting mounds where similar redox and hydrologic conditions are expected.

In this study, T-RFLP as well as traditional clone library and sequencing methods were used to track the spacial variability, community composition, and comparatively fingerprint microbial communities within a sediment core collected from an off-axis hydrothermally active mound on the Cleft Segment of the southern Juan de Fuca Ridge. This is the first study to determine the microbial composition of a hydrothermal mound located on the southern Juan de Fuca Ridge using molecular microbial methods. This is also the first study to identify a microbial community dominated by the  $\zeta$ -*Proteobacteria* in hydrothermal sediment, although the tight T-RFLP clustering between the microbial communities from the center of the mound with multiple iron-dominated microbial mat communities indicates that this group may be a common dominant member of microbial communities from hydrothermal systems in which hydrothermal fluids containing high concentrations of iron and/or manganese upwell through sediment deposited over young basaltic crust.

The large Fe-Mn-Si-rich mound that we sampled is likely structurally controlled by the ridge parallel fault and may be directly associated with off-axis volcanism and associated hydrothermal circulation rather than being connected to axial hydrothermal circulation (Stakes et al. 2006). Given the large amount of heat and fluid flux that must occur in this near but off-axis setting (Mottl 2003) our results demonstrate that there is great potential for diffuse hydrothermal flow to occur at significant distances from the axis, creating low-temperature Fe-, Si-, and Mn-rich deposits that harbor microbial communities that in part shape their habitat through the precipitation of oxides.

## REFERENCES

- Altschul SF, Gish W, Miller W, Myers EW, Lipman DJ. 1990. Basic local alignment search tool. *J Mol Biol* 215:403–410.
- Ashelford KE, Chuzhanova NA, Fry JC, Jones AJ, Weightman AJ. 2005. At least 1 in 20 16S rRNA sequence records currently held in public repositories is estimated to contain substantial anomalies. *Appl Environ Microbiol* 71:7724–7736.
- Bowman JD, Sly LI, Stackebrandt E. 1995. The phylogenetic position of the family *Methylococcaceae*. *Int J Syst Bacteriol* 45:182–185.
- Brendel PJ, Luther GW. 1995. Development of a gold amalgam voltammetric microelectrode for the determination of dissolved Fe, Mn, O<sub>2</sub>, and S(-II) in porewaters of marine and freshwater sediments. *Environ Sci Technol* 29:751–761.
- Chadwick WW, Embley RW. 1994. Lava flows from a mid-1980s submarine eruption on the Cleft segment, Juan de Fuca Ridge. *J Geophys Res* 99:4761–4776.
- Chao A. 1984. Non-parametric estimation of the number of classes in a population. *Scand J Stat* 11:265–270.
- Davis RE, Moyer CL. 2008. Extreme spatial and temporal variability of hydrothermal microbial mat communities along the Mariana Island Arc and southern Mariana back-arc system. *J Geophys Res* 113:B08S15, doi:10.1029/2007JB005413.
- Devereux R, Mundfrom GW. 1994. A phylogenetic tree of 16S rRNA sequences from sulfate-reducing bacteria in a sandy marine sediment. *Appl Environ Microbiol* 60:3437–3439.
- Dhillon A, Teske A, Dillon J, Stahl DA, Sogin ML. 2003. Molecular characterization of sulfate-reducing bacteria in the Guaymas Basin. *Appl Environ Microbiol* 69:2765–2772.
- Eder W, Jahnke LL, Schmidt M, Huber R. 2001. Microbial diversity of the brine-seawater interface of the Kebrut Deep, Red Sea, studied via 16S rRNA gene sequences and cultivation methods. *Appl Environ Microbiol* 67:3077–3085.
- Edwards KJ, Bach W, McCollom TM. 2005. Geomicrobiology in oceanography: microbe-mineral interactions at and below the seafloor. *Trends Microbiol* 13:449–456.
- Edwards KJ, Rogers DR, Wirsén CO, McCollom TM. 2003. Isolation and characterization of novel psychrophilic, neutrophilic, Fe-oxidizing, chemolithoautotrophic  $\alpha$ - and  $\gamma$ -Proteobacteria from the deep sea. *Appl Environ Microbiol* 69:2906–2913.
- Embley RW, Chadwick WW. 1994. Volcanic and hydrothermal processes associated with a recent phase of seafloor spreading at the northern Cleft segment: Juan de Fuca Ridge. *J Geophys Res* 99:4741–4760.
- Embley RW, Hammond SR, Malahoff A, Ryan WBF, Crane K, Kappel E. 1983. Rifts of the southern Juan de Fuca. *Eos Trans AGU* 64:853.
- Emerson D, Moyer CL. 1997. Isolation and characterization of novel iron-oxidizing bacteria that grow at circumneutral pH. *Appl Environ Microbiol* 63:4784–4792.
- Emerson D, Moyer CL. 2002. Neutrophilic Fe-oxidizing bacteria are abundant at the Loihi Seamount hydrothermal vents and play a major role in Fe oxide deposition. *Appl Environ Microbiol* 68:3085–3093.
- Emerson D, Rentz JA, Lilburn TG, Davis RE, Aldrich H, Chan C, Moyer CL. 2007. A novel lineage of Proteobacteria involved in formation of marine Fe-oxidizing microbial mat communities. *PLoS ONE* 2:e667; doi:10.1371/journal.pone.0000667.
- Emerson D, Revsbech NP. 1994. Investigation of an iron-oxidizing microbial mat community located near Aarhus, Denmark: field studies. *Appl Environ Microbiol* 60:4022–4031.
- Engelbreton JJ, Moyer CL. 2003. Fidelity of select restriction endonucleases in determining microbial diversity by terminal-restriction fragment length polymorphism. *Appl Environ Microbiol* 69:4823–4829.
- Fitzgerald CE, Gillis KM. 2006. Hydrothermal manganese oxide deposits from Baby Bare seamount in the Northeast Pacific Ocean. *Mar Geol* 225:145–156.
- Hall TA. 1999. BioEdit: A user-friendly biological sequence alignment editor and analysis program for Windows 95/98/NT. *Nucl Acids Symp Ser* 41:95–98.
- Häne BG, Jäger K, Drexler HG. 1993. The Pearson product-moment correlation coefficient is better suited for identification of DNA fingerprint profiles than band matching algorithms. *Electrophoresis* 14, 967–972.
- Haymon RM, Macdonald KC, Benjamin SB, Ehrhardt CJ. 2005. Manifestations of hydrothermal discharge from young abyssal hills on the fast-spreading East Pacific Rise flank. *Geology* 33:153–156.
- Huber JA, Johnson HP, Butterfield DA, Baross JA. 2006. Microbial life in ridge flank crustal fluids. *Environ Microbiol* 8:88–99.
- Huber T, Faulkner G, Hugenholtz P. 2004. Bellerophon: a program to detect chimeric sequences in multiple sequence alignments. *Bioinformatics* 20:2317–2319.
- Karl DM, McMurtry GM, Malahoff A, Garcia MO. 1988. Loihi Seamount, Hawaii: a mid-plate volcano with a distinctive hydrothermal system. *Nature* 335:532–535.
- Kennedy CB, Scott SD, Ferris FG. 2003a. Characterization of bacteriogenic iron oxide deposits from Axial Volcano, Juan de Fuca Ridge, northeast Pacific Ocean. *Geomicrobiol J* 20:199–214.

- Kennedy C, Scott S, Ferris F. 2003b. Ultrastructure and potential sub-seafloor evidence of bacteriogenic iron oxides from Axial Volcano, Juan de Fuca Ridge, north-east Pacific Ocean. *FEMS Microbiol Ecol* 43:247–254.
- Kishino H, Hasegawa M. 1989. Evaluation of the maximum likelihood estimate of the evolutionary tree topologies from DNA sequence data, and the branching order in *Hominoidea*. *J Mol Evol* 29:170–179.
- Kucera S, Wolfe RS. 1957. A selective enrichment method for *Gallionella ferruginea*. *J Bacteriol* 74:344–349.
- Li L, Kato C, Horikoshi K. 1999. Bacterial diversity in deep-sea sediments from different depths. *Biodivers Conserv* 8:659–677.
- Liu WT, Marsh TL, Cheng H, Forney LJ. 1997. Characterization of microbial diversity by determining terminal restriction fragment length polymorphisms of genes encoding 16S rRNA. *Appl Environ Microbiol* 63:4516–4522.
- Lovley DR. 1997. Microbial Fe(III) reduction in subsurface environments. *FEMS Microbiol Rev* 20:305–313.
- Ludwig W, Strunk O, Westram R, Richter L, Meier H, Kumar Y, Buchner A, Lai T, Steppi S, Jobb G, Förster W, Brettske I, Gerber S, Ginhart AW, Gross O, Grumann S, Hermann S, Jost R, König A, Liss T, Lüßmann R, May M, Nonhoff B, Reichel B, Strehlow R, Stamatakis A, Stuckmann N, Vilbig A, Lenke M, Ludwig T, Bode A, Schleifer KH. 2004. ARB: a software environment for sequence data. *Nucl Acids Res* 32:1363–1371.
- Massoth GJ, Baker ET, Lupton JE, Feely RA, Butterfield DA, Von Damm KL, Roe KK, Lebon GT. 1994. Temporal and spatial variability of hydrothermal manganese and iron at Cleft segment, Juan de Fuca Ridge. *J Geophys Res* 99:4905–4923.
- Mottl MJ. 2003. Partitioning of energy and mass fluxes between mid-ocean ridge axes and flanks at high and low temperature. In *Energy and Mass Transfer in Marine Hydrothermal Systems* (PE Halbach, V Tunnicliffe, JR Hein, eds.), pp. 271–286. Dahlem University Press, Berlin.
- Moyer CL. 2001. Molecular phylogeny: applications and implications for marine microbiology. *Meth Microbiol* 30:375–394.
- Moyer CL, Dobbs FC, Karl DM. 1995. Phylogenetic diversity of the bacterial community from a microbial mat at an active, hydrothermal vent system, Loihi Seamount, Hawaii. *Appl Environ Microbiol* 61:1555–1562.
- Olsen GJ, Matsuda H, Hagstrom R, Overbeek R. 1994. fastDNAm1: a tool for construction of phylogenetic trees of DNA sequences using maximum likelihood. *Comput Appl Biosci* 10:41–48.
- Santelli CM, Orcutt BN, Banning E, Bach W, Moyer CL, Sogin ML, Staudigel H, Edwards, KJ. 2008. Abundance and diversity of microbial life in ocean crust. *Nature* 453:653–656.
- Schloss PD, Handelsman J. 2005. Introducing DOTUR, a computer program for defining operational taxonomic units and estimating species richness. *Appl Environ Microbiol* 71:1501–1506.
- Schrenk MO, Kelley DS, Delaney JR, Baross JA. 2003. Incidence and diversity of microorganisms within the walls of an active deep-sea sulfide chimney. *Appl Environ Microbiol* 69:3580–3592.
- Stakes DS, Perfit MR, Wheat CG, Ramirez TM, Koski RA, Hein JR. 2003. Evidence of off-axis volcanism and hydrothermal venting along the Cleft segment of the southern Juan de Fuca Ridge. *Geophys Res Abstr* 5:EGS/AGU/EUG Jt. Assem., Abstract EAE03-A-04666.
- Stakes DS, Perfit MR, Tivey MA, Caress DW, Ramirez TM, Maher N. 2006. The Cleft revealed: Geologic, magnetic, and morphologic evidence for construction of upper oceanic crust along the southern Juan de Fuca Ridge. *Geochem. Geophys. Geosyst.* 7, Q04003, doi:10.1029/2005GC001038.
- Takai K, Komatsu T, Inagaki F, Horikoshi K. 2001. Distribution of archaea in a black smoker chimney structure. *Appl Environ Microbiol* 67:3618–3629.
- Tebo BM, Johnson HA, McCarthy JK, Templeton AS. 2005. Geomicrobiology of manganese(II) oxidation. *Trends Microbiol* 13:421–428.
- Templeton A, Staudigel H, Tebo BM. 2005. Diverse Mn(II)-oxidizing bacteria isolated from submarine basalts at Loihi Seamount. *Geomicrobiol J* 22:127–139.
- Teske A, Alm E, Regan JM, Toze S, Rittmann BE, Stahl DA. 1994. Evolutionary relationships among ammonia- and nitrite-oxidizing bacteria. *J Bact* 176:6623–6630.
- Von Damm KL, Edmond JM, Grant B, Measures CI, Walden B, Weiss RF. 1985. Chemistry of submarine hydrothermal systems at 21°N, East Pacific Rise. *Geochim. Cosmochim Acta* 49:2197–2220.
- Watson SW, Waterbury JB. 1971. Characteristics of two marine nitrite oxidizing bacteria, *Nitrospina gracilis* nov. gen. nov. sp. and *Nitrococcus mobilis* nov. gen. nov. sp. *Arch Microbiol* 77:203–230.